Colloids and Surfaces A: Physicochemical and Engineering Aspects 652 (2022) 129813

Contents lists available at ScienceDirect

Colloids and Surfaces A: Physicochemical and Engineering Aspects

journal homepage: www.elsevier.com/locate/colsurfa

Turn-on fluorescence of davydov-split aggregate particles for protein detection

Yiping Ma, Arianna Dicce, Nitin Ramesh Reddy, Jiyu Fang *

Department of Materials Science and Engineering and Advanced Materials Processing and Analysis Center, University of Central Florida, Orlando, Florida 32816, USA

GRAPHICAL ABSTRACT

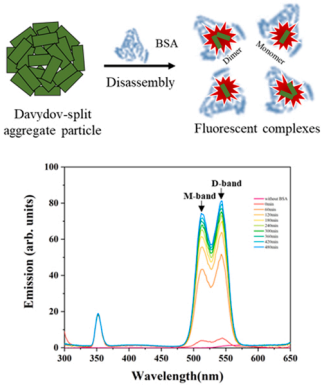

ARTICLE INFO

Keywords:
Cyanine dyes
Proteins
Davydov-split aggregates
Disassembly
Turn-on fluorescence
Detection

ABSTRACT

The turn-on fluorescence of supramolecular aggregates of organic dyes through the interaction with specific proteins is highly desirable for the development of a high signal-to-noise fluorescence probe for biomedical applications. In this paper, we use the self-assembly of 3,3′-ditetradecyloxacarbocyanine ($DiOC_{14}(3)$) in the methanol/water mixture with/without NaOH to form Davydov-split aggregate particles. We show that the crystalline Davydov-split aggregate particles formed in the presence of NaOH failed to respond to bovine serum albumin (BSA). While the non-crystalline Davydov-split aggregate particles formed in the absence of NaOH gradually disassembled through the interaction with BSA. The disassembled $DiOC_{14}(3)$ molecules complex with BSA in the monomer and twisted H-dimer forms, consequently turning on fluorescence. The turn-on fluorescence is highly specific to BSA and linearly increases with the increase of BSA concentrations. Furthermore, we show that the turn-on fluorescence behavior of non-crystalline Davydov-split aggregate particles by BSA can also be achieved in synthetic urine, which highlights their potential for the detection of urinary albumin.

* Corresponding author.
E-mail address: Jiyu.fang@ucf.edu (J. Fang).

https://doi.org/10.1016/j.colsurfa.2022.129813
Received 30 June 2022; Received in revised form 25 July 2022; Accepted 25 July 2022
Available online 27 July 2022

1. Introduction

Cyanine dyes are an ionic compound containing two nitrogen-containing heterocyclic rings linked by a conjugated polymethine backbone [1]. They have been widely used for bioimaging and biosensing due to their high absorption coefficient, strong fluorescence emission, and low toxicity [2–5]. In addition, the optical properties of cyanine dyes can be simply tuned by chemically modifying their conjugated backbones and heterocyclic rings [6]. Although cyanine dyes have merits as fluorescent probes, they may suffer from relatively high background fluorescence and low aqueous solubility.

There is a need for the development of novel fluorescent probes for biomedical applications. Recently, the non-fluorescent nanoparticles formed by squaraine, tetraphenylethylene, and coumarin derivatives have received interest because of their low background fluorescence [7–11]. It has been shown that the turn-on fluorescence through the disassembly of the non-fluorescent nanoparticles is highly sensitive and selective for serum albumin proteins. In addition, the non-fluorescent nanoparticles can efficiently penetrate into cell membranes, providing the possibility of detecting serum albumin proteins in cells with a high signal-to-noise ratio [10,11].

It is well known that cyanine dyes have the tendency of assembling into highly ordered supramolecular aggregates [12]. The exciton delocalization in the supramolecular aggregates gives rise to unique physical properties. For example, J-aggregates, in which the transition dipole moments of cyanine dyes are parallel to each other in a head-to-tail arrangement, show a red-shifted absorbance band (J-band) with respect to the monomer band and a strong fluorescence emission [13]. In contrast, H-aggregates, in which the transition dipole moments of cyanine dyes are parallel in a face-to-face arrangement, show a blue-shifted absorbance band (H-band) with respect to the monomer band and a very weak fluorescence [14]. Davydov-split aggregates, in which the transition dipole moments of cyanine dyes are twisted to each other, show a H-band and a J-band because optical energy transitions to both the lower and high energy excited states are allowed [15]. The fluorescence mission of Davydov-split aggregates depends on the twisted angle of the transition dipole moments of cyanine dyes [16–18]. Recently, Davydov-split aggregates of cyanine dyes have been used in chiroptical detection [19] and artificial light-harvesting [20,21].

The understanding of the turn-on fluorescence behavior of these highly ordered supramolecular aggregates in response to specific proteins is critical for validating their potential as a fluorescent probe for biomedical applications. Recently, the interaction of J- and H-aggregates of a cyanine derivative with human serum albumin (HSA) was reported in the literature [22]. The disassembly of the J- and H-aggregates into monomers through the interaction with HSA produced the detectable changes in color and fluorescence. In this paper, we formed Davydov-split aggregate particles by the self-assembly of 3,3′-ditetradecyloxacarbocyanine ($DiOC_{14}(3)$) in the methanal/water mixture with/without NaOH. The interaction of the Davydov-split aggregate particles with bovine serum albumin (BSA) was investigated by UV–vis absorption and fluorescence spectroscopies. We found that the crystalline Davydov-split aggregate particles formed in the presence of NaOH failed to respond to BSA. While the non-crystalline Davydov-split aggregate particles formed the absence of NaOH gradually disassembled through the interaction of BSA, consequently turning on two fluorescence bands. One was associated with the monomer complexed with BSA and other was associated with the twisted H-dimer complexed with BSA. The intensity of the turn-on fluorescence of the monomer and twisted H-dimers showed a linear response over the certain concentration range of BSA. Furthermore, the turn-on fluorescence behavior of non-crystalline Davydov-split aggregate particles by BSA was studied in synthetic urine.

2. Experimental section

2.1. Materials

3,3′-ditetradecyloxacarbocyanine ($DiOC_{14}(3)$), bovine serum albumin, lysozyme, trypsin, and hemoglobin, were purchased from Sigma-Aldrich and used without further purification. Sodium hydroxide (NaOH) and methanol were from Sigma-Aldrich. Synthetic urine was purchased from Sigma-Aldrich and diluted by 100 times before being used. Deionized water (18 MΩ cm, pH 5.7) was obtained from Easypure II system.

2.2. Formation of Davydov-split aggregate particles

$DiOC_{14}(3)$ was dissolved in 2 mL methanol at 55 °C for forming stock solution. The stock solution was then mixed with 2 mL water with the final $DiOC_{14}(3)$ concentration of 0.5 mM in the presence and absence of sodium hydroxide (NaOH). The mixed solution was sonicated at ~50 °C in an ultrasonic bath (Branson 1510, Branson Ultrasonics Co.) for 5 min and then cooled to room temperature. After the mixed solution was aged at room temperature for 24 h, a color change was observed, suggesting the formation of aggregates of $DiOC_{14}(3)$. The aggregate solution was stored in the dark when not in use.

2.3. Characterizations

UV-Vis absorbance spectra were recorded at room temperature with Cary 60 UV–vis spectrophotometer using a 10-mm cuvette. Fluorescence spectra were recorded at the synchronous mode with $\Delta = 40$ nm with Jasco FP-6500 spectrofluorometer. Optical microscopy images were taken with an Olympus BX40 microscope. Dynamic light scattering was measured with a Zetasizer Nano ZS90 (Malvern Instruments Inc.).

2.4. BSA detection in synthetic urine with Davydov-split aggregate particles

The solution of Davydov-split aggregate particles was then diluted by 25 times and 250 times with the diluted synthetic urine, followed by the addition of BSA with different concentrations. After 4 h incubation, the absorption and fluorescence emission spectra were taken for each BSA concentrations at room temperature.

3. Results and discussion

3,3′-ditetradecyloxacarbocyanine ($DiOC_{14}(3)$) is a lipophilic fluorescent dye with a conjugated polymethine backbone and two alkyl tails bearing 14 carbons (Fig. 1a). 2 μM $DiOC_{14}(3)$ in methanol showed a monomer absorption band at 485 nm with a short wavelength shoulder band at 460 nm (Fig. 1b). The short wavelength shoulder band could be assigned to H-dimers [23,24]. The fluorescence spectrum of 2 μM $DiOC_{14}(3)$ in methanol showed the mirror image of the absorption spectrum (Fig. 1b). The strong fluorescence at 505 nm with the small Stokes shift of 20 nm could be assigned to the monomer emission. 2 μM $DiOC_{14}(3)$ in water showed a strong H-dimer band at 460 nm (Fig. 1c). In this case, the monomer band at 485 nm was weak and appeared as a shoulder. This result suggested that the majority of $DiOC_{14}(3)$ molecules formed H-dimers in water. The H-dimes showed a very weak fluorescence at 556 nm (Fig. 1c), suggesting the parallel arrangement of the transition dipole moments of $DiOC_{14}(3)$ molecules in the H-dimer.

In a previous publication, we showed that the addition of water in the methanol solution of $DiOC_{14}(3)$ could lead to the formation of Davydov-split aggregates [25]. Fig. 2a shows the absorption spectrum of 0.5 mM $DiOC_{14}(3)$ in the methanol/water mixture (1:1, v/v), in which a large blue-shifted H-band at 400 nm and a small red-shifted J-band at 524 nm with respect to the monomer band were observed, referred as Davydov-splitting. The Davydov-splitting between the H-band and the

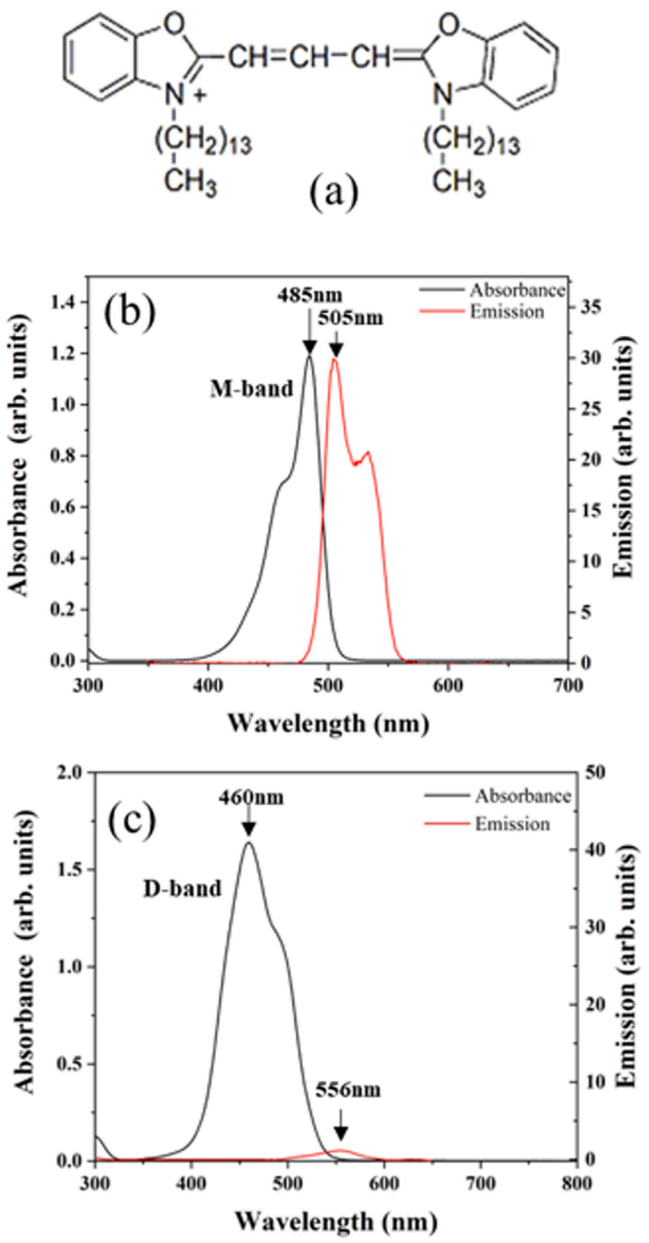

Fig. 1. (a) Chemical structure of $DiOC_{14}(3)$. UV-Vis absorption and fluorescence spectra of 2 μM $DiOC_{14}(3)$ in methanol (b) and in water (c).

J-band was 124 nm and asymmetric with respect the monomer band. The intensity of the H-band was slightly lower than that of the J-band. Optical microscopy images revealed that the size of Davydov-split aggregates was in microns (Fig. 2b). The microsized Davydov-split aggregate particles showed no birefringence when being viewed under crossed polarizers, suggesting that there was no long-range ordering of $DiOC_{14}(3)$ molecules in the aggregate particles (referred as non-crystalline phase). In the methanol/water mixture (1:1, v/v) with 3 mM NaOH, the formation of Davydov-split aggregates of $DiOC_{14}(3)$ was also observed (Fig. 2c), in which the H-band appeared at 418 nm and the J-band was at 515 nm with the Davydov-splitting of 97 nm. The intensity of the H-band was slightly higher than that of the J-band. In this case, the Davydov-split aggregate particles showed a birefringent Maltese-cross pattern when being viewed under crossed polarizers (Fig. 2d), suggesting that the $DiOC_{14}(3)$ molecules have a long-range ordering in the aggregate particles (referred as a crystalline phase).

The aggregation of $DiOC_{14}(3)$ molecules in the methanol/water mixture was driven by hydrophobic, electrostatic, and π-π interactions. In the presence of NaOH, the charge of $DiOC_{14}(3)$ molecules might be screeded by OH^- ions, reducing their electrostatic repulsion. Thus, the hydrophobic and π–π attractions of $DiOC_{14}(3)$ molecules were the main driving force for the formation of the crystalline Davydov-split aggregate particles.

Serum albumin is a major protein in blood plasma, which shows the excellent ability of binding to various ligands [26,27]. The interaction of serum albumin with cyanine dyes has been extensively studied due to the interest in developing new fluorescent probes. It has been shown that the binding of cyanine dyes in the hydrophobic cavities of serum albumin can significantly improve their aqueous solubility, quantum yield, and in vivo circulation time due to the change of their local environments [28–32]. In our experiments, the interaction of Davydov-split aggregate particles with bovine serum albumin (BSA) was studied, in which the solution of Davydov-split aggregate particles was diluted by 25 times with water and then incubated with 12 μM BSA. There was no change in the absorption spectrum of the crystalline and non-crystalline Davydov-split aggregate particles after 25-time dilution. As could be seen in Fig. 3a, the fluorescence of the crystalline Davydov-split aggregate particles was largely quenched. After the addition of 12 μM BSA, a strong fluorescence band at 352 nm, which corresponded to the fluorescence emission of the tryptophan residue of BSA, was observed (Fig. 3a). However, the crystalline Davydov-split aggregate particles showed no fluorescence enhancement after 4 h incubation with BSA. In addition, polarizing optical images showed that there was no disruption in the birefringent Maltese-cross pattern of crystalline Davydov-split aggregate particles (Fig. 3b). These results suggested that the interaction of $DiOC_{14}(3)$ and BSA at the surface of the crystalline Davydov-split aggregate particles was not able to disrupt the arrangement of $DiOC_{14}(3)$ molecules in the particles.

On the other hand, we found that the non-crystalline Davydov-split aggregate particles responded to 1 μM BSA by changing their absorption and fluorescence spectra. Fig. 4a shows the absorption spectra of the non-crystalline Davydov-split aggregate particles after the addition of BSA in the concentration range from 1 μM to 9 μM, in which the H-band at 400 nm and the J-band at 524 nm disappeared. Instead, we observed a monomer band at 497 nm and a H-dimer band at 467 nm, suggesting that the non-crystalline Davydov-split aggregate particles disassembled into monomers and H-dimers. The absorption band of the monomer and H-dimer red shifted with respect to that of the free monomer and H-dimer shown in Fig. 1b and c, respectively. The red-shifted absorption bands were a result of the binding of the monomer and H-dimer in the hydrophobic cavity of BSA to form the monomer/BSA and H-dimer/BSA complexes. Fig. 4b shows the fluorescence spectra of the non-crystalline Davydov-split aggregate particles before and after the addition of BSA. The non-crystalline Davydov-split aggregate particles showed weak fluorescence with a maximum at 570 nm. After the addition of 1 μM BSA, the weak fluorescence at 570 nm disappeared, which suggested the disassembly of the non-crystalline Davydov-split aggregate particles through the interaction with BSA. At the same time, we observed two new fluorescence bands at 519 nm and 543 nm (Fig. 4b), which could be assigned to the emission of the monomer and H-dimer complexed with BSA, respectively. It has been shown that the fluorescence of H-dimers and H-aggregates may arise from the twisted arrangement of dye molecules [21,33,34]. The α-helix is the most abundant conformation of BSA. The helical J-aggregates of dyes induced by the α-helix of HSA was reported in the literature [28,35]. Thus, we inferred that the interaction of H-dimers with the α-helix of BSA induced a twisted arrangement of $DiOC_{14}(3)$ molecules, consequently turning on the fluorescence at 543 nm. This result showed that BSA not only complexed with the disassembled $DiOC_{14}(3)$ molecules but also induced the twisted H-dimers. The intensity of the twisted H-dimer and the monomer emissions linearly increased with the increase of the BSA concentrations from 1 μM to 9 μM (Fig. 4c and d), suggesting that the positive correlations between the concentration of BSA with the amount of the monomeric and the

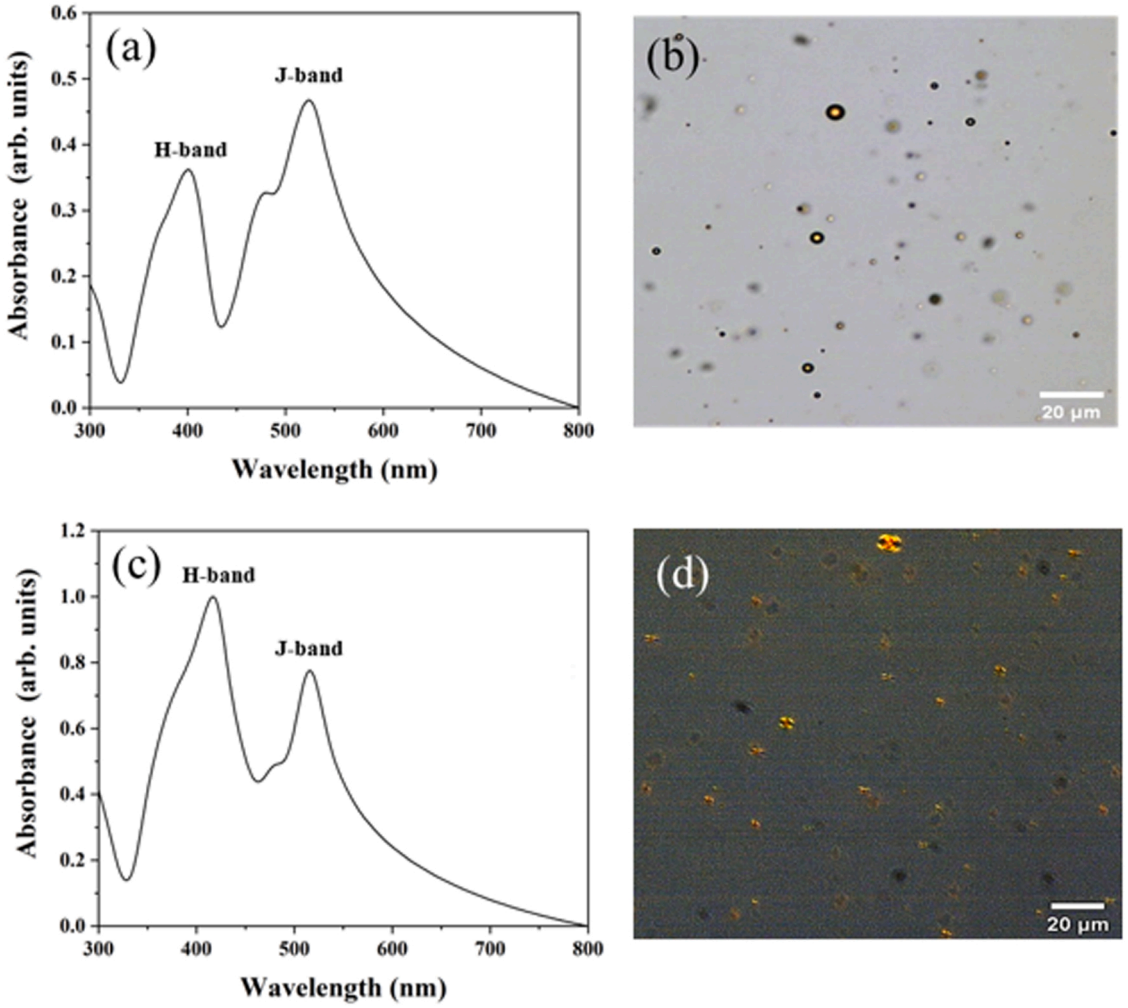

Fig. 2. (a) UV-Vis absorption spectra of 0.5 mM $DiOC_{14}(3)$ in the methanol/water mixture (1:1, v/v) after being aged for 24 h. (b) Optical microscopy image of Davydov-split aggregate particles in the absence of NaOH. (c) UV-Vis absorption spectra of 0.5 mM $DiOC_{14}(3)$ in the methanol/water mixture (1:1, v/v) with 3 mM NaOH after being aged for 24 h. (d) Polarizing microscopy image of Davydov-split aggregate particles formed in the presence of 3 mM NaOH.

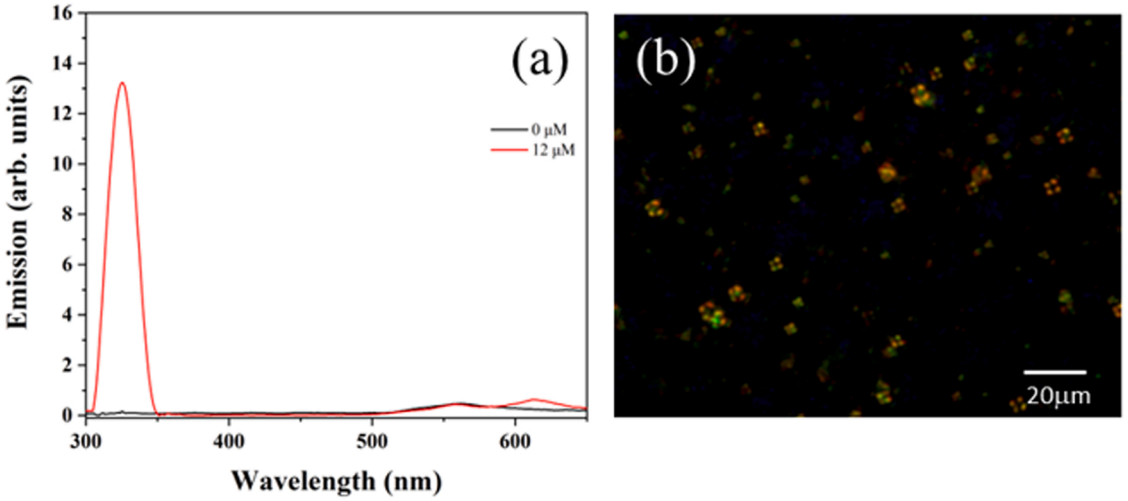

Fig. 3. (a) Fluorescence emission spectra of crystalline Davydov-split aggregate particles before and after 4 h incubation with 12 μM BSA. The solution of aggregate particles was diluted by 25 times with water. (b) Polarizing microscopy image of crystalline Davydov-split aggregate particles after 4 h incubation with 12 μM BSA.

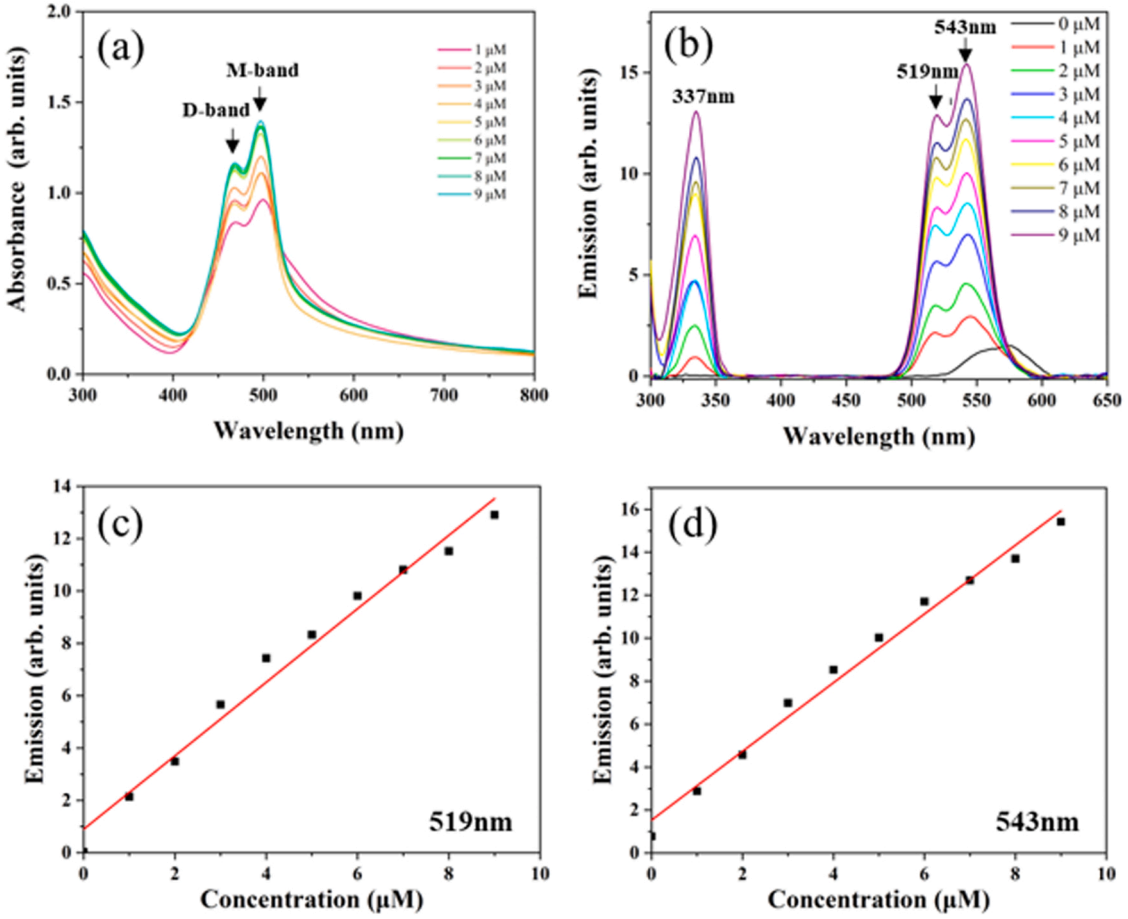

Fig. 4. (a) Absorption and (b) fluorescence emission spectra of non-crystalline Davydov-split aggregate particles after the addition of BSA with different concentrations. The solution of aggregate particles was diluted by 25 times with water. Each spectrum was taken after 4 h incubation with BSA. The plot of the intensity of the turn-on fluorescence emission at 519 nm (b) and 543 nm (c) as a function of BSA concentrations.

dimeric $DiOC_{14}(3)$.

The disassembly of the non-crystalline Davydov-split aggregate particles through the interaction with BSA was further confirmed by dynamic light scattering. The non-crystalline Davydov-split aggregate particles showed a broad size distribution with the two maximums at 0.7 μm and 2.5 μm (Fig. 5a). After the addition of 12 μM BSA, the significantly reduced size of the non-crystalline Davydov-split aggregate particles was observed (Fig. 5b). Thus, the turn-on fluorescence mechanism of non-crystalline Davydov-split aggregate particles through the interaction with BSA was shown in Fig. 5c. It was reported that the binding between cyanine dyes and BSA was mainly driven by the hydrophobic and electrostatic interactions [28], which were likely responsive for the disassembly of the non-crystalline Davydov-split aggregate particles. The disassembled $DiOC_{14}(3)$ molecules then complex with BSA in the monomer and twisted H-dimer forms, consequently showing the turn-on fluorescence at 519 nm and 543 nm, respectively.

To have a better understanding of the disassembly of non-crystalline Davydov-split aggregate particles through the interaction with BSA, we measured the time-dependent fluorescence spectra of non-crystalline Davydov-split aggregate particles after the addition of 80 μM BSA, which showed that both the monomer and twisted H-dimer emissions increased over time (Fig. 6a). Since there was no isosbestic point in the fluorescence spectra, we might infer that the disassembled $DiOC_{14}(3)$ molecules formed both the monomer/BSA and twisted H-dimer/BSA complexes. Fig. 6b shows the plot of the intensity of the monomer and twisted H-dimer missions as a function of time, which revealed that the disassembly of non-crystalline Davydov-split aggregate particles was relatively fast within the first 100 min and then gradually approached to the equilibrium over time. It was also clear in Fig. 6b that the intensity of the monomer and twisted H-dimer missions increased simultaneously over time, suggesting that the formation ratio of the monomer/BSA complex was the same as that of the twisted H-dimer/BSA complex.

Finally, we studied the turn-on fluorescence behavior of non-crystalline Davydov-split aggregate particles by BSA in synthetic urine, which contains urea, sodium chloride, magnesium sulfate heptahydrate, and calcium chloride dehydrate. In our experiments, the solution of non-crystalline Davydov-split aggregate particles was diluted by 25 times with synthetic urine. After the dilution, the J-band position of Davydov-split aggregate particles remained unchanged, while the H-band shifted from 400 nm to 474 nm. In this case, the Davydov-splitting was reduced to 41 nm, suggesting that the separation of $DiOC_{14}(3)$ molecules in the aggregate particles was enlarged in synthetic urine [15]. After the addition of 3 μM BSA, the J-band at 524 nm and the H-band at 474 nm disappeared, suggesting the disassembly of the aggregate particles. At the same time, a monomer band at 492 and H-dimer shoulder band at 466 nm were observed (Fig. 7a). The intensity of both the monomer and H-dimer absorption bands increased with the increase of BSA concentrations from 3 μM to 10 μM. Before the addition of BSA, the non-crystalline Davydov-split aggregate particles in synthetic urine showed a weak fluorescence at 570 nm (Fig. 7b). After the disassembly of the non-crystalline Davydov-split aggregate particles through the interaction with BSA, the H-dimer complexed with BSA showed a strong emission at 535 nm due to the twisted arrangement of $DiOC_{14}(3)$ molecules. In this case, the emission of the monomer complexed with BSA was relatively weak and appeared as a shoulder at 517 nm (Fig. 7b). The intensity of the twisted H-dimer emission at

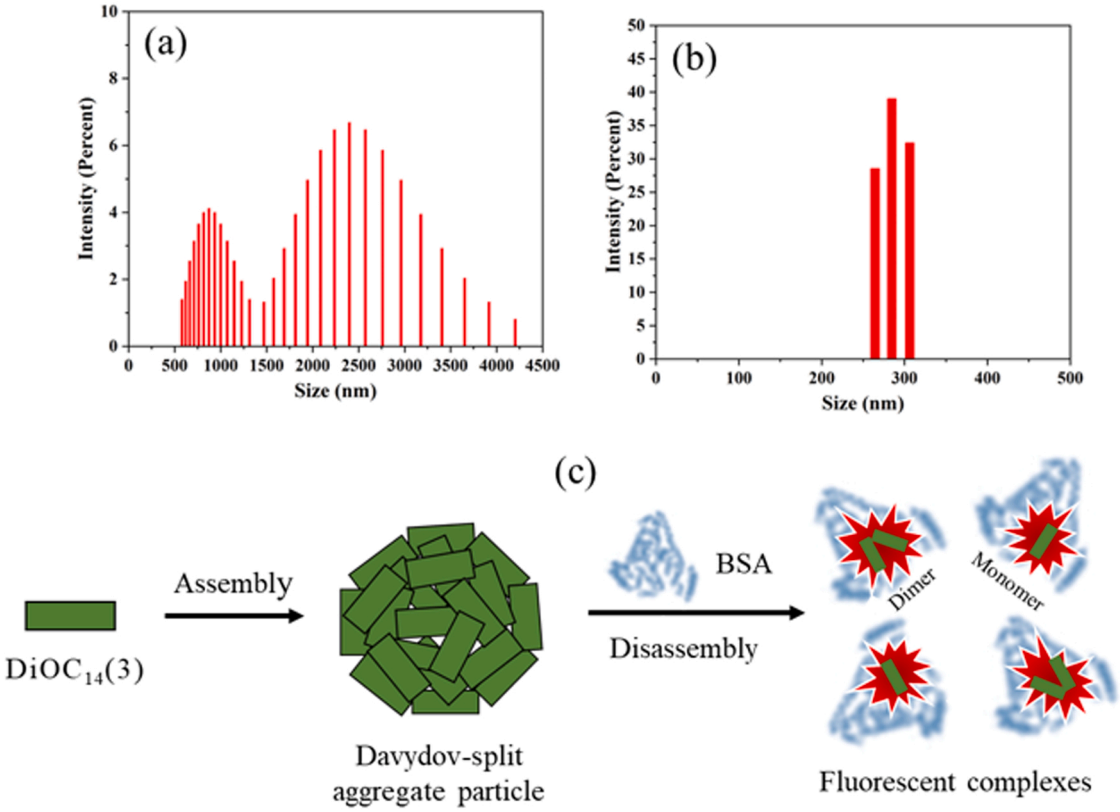

Fig. 5. Dynamic light scattering analysis of non-crystalline Davydov-split aggregate particles before (a) and after (b) addition of 12 μM BSA (1 h incubation). The solution of aggregate particles was diluted by 25 times with water. (c) Schematic illustration of the assembly and disassembly of Davydov-split aggregate particles and the turn-on fluorescence from the monomer and twisted H-dimer complexed with BSA.

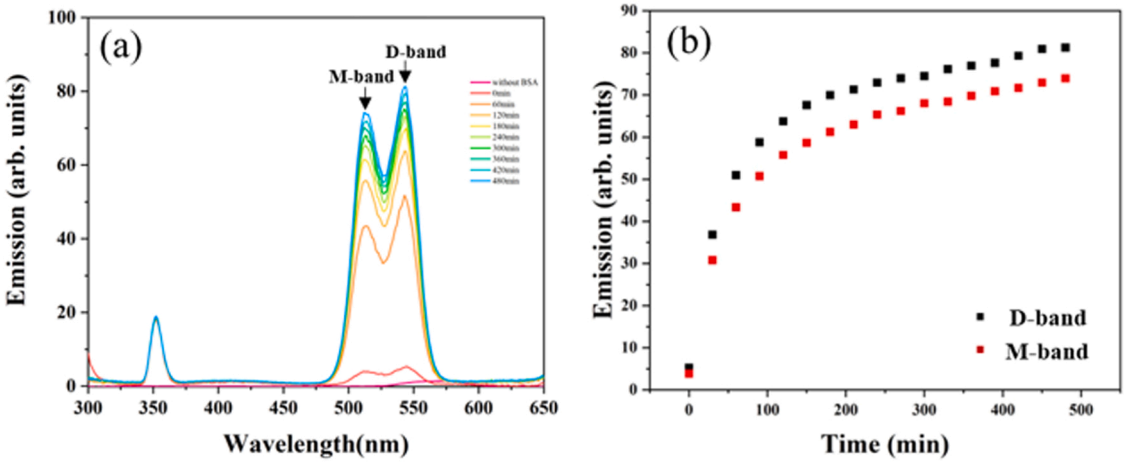

Fig. 6. (a) Time-dependent fluorescence emission spectra of non-crystalline Davydov-split aggregate particles after the addition of 80 μM BSA. The solution of aggregate particles was diluted by 25 times with water. Each fluorescence spectrum was taken after 4 h incubation with BSA. (b) The plot of the intensity of the turn-on fluorescence emission at 519 nm (M-band) and 543 nm (D-band) as a function of time.

535 nm linearly increased over the BSA concentration range from 3 μM to 10 μM (Fig. 7c), suggesting that the turn-on fluorescence of the non-crystalline Davydov-split aggregate particles might have the potential for quantifying BSA. The detection limit of the non-crystalline Davydov-split aggregate particles for BSA was estimated by multiplying the ratio of the standard deviation to the slope of the linear fit curve by 3.3 to be ~ 0.6 μM.

To verify the selectivity of non-crystalline Davydov-split aggregate particles, lysozyme, trypsin, and hemoglobulin with the same concentration (12 μM) were used in our experiments. However, none of these proteins was able to turn on the fluorescence of non-crystalline Davydov-split aggregate particles (Fig. 7d). The selective response of non-crystalline Davydov-split aggregate particles toward BSA could be attributed to the highly specific binding between BSA and $DiOC_{14}(3)$. The result confirms the feasibility of Davydov-split aggregate particles as a probe for the selective detection of BSA.

Interestingly, when the solution of non-crystalline Davydov-split aggregate particles was diluted by 250 times with synthetic urine, they were able to response to BSA in the nanomolar level. In this case, the Davydov-split aggregate particles showed a J-band at 524 nm and a H-

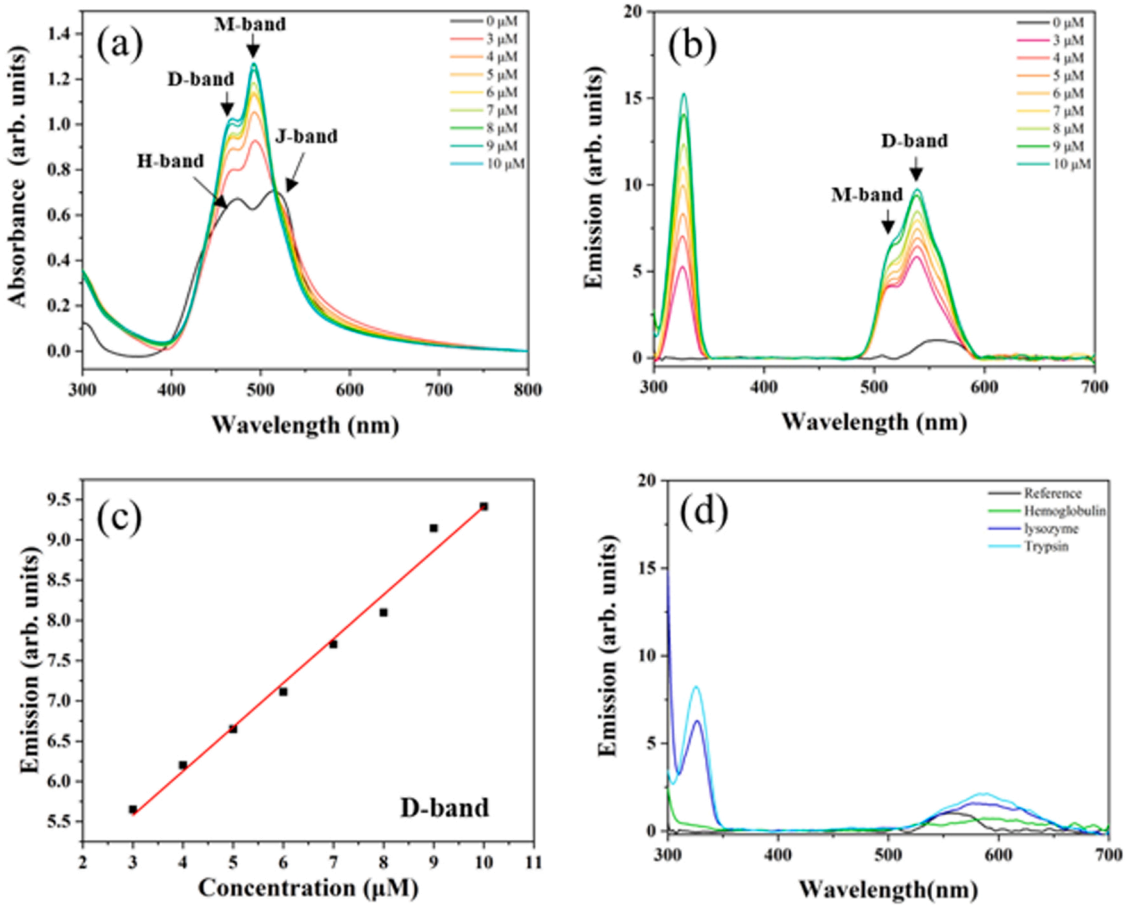

Fig. 7. (a) UV–vis absorption and (b) fluorescence emission spectra of non-crystalline Davydov-split aggregate particles before and after the addition of BSA with different concentrations. The solution of aggregate particles was diluted by 25 times with synthetic urine. Each fluorescence spectrum was taken after 4 h incubation with BSA. (c) The plot of the intensity of the turn-on fluorescence at 543 nm as a function of BSA concentrations. (d) Fluorescence spectra of non-crystalline Davydov-split aggregate particles before and after the addition of 12 μM hemoglobulin, lysozyme, and trypsin.

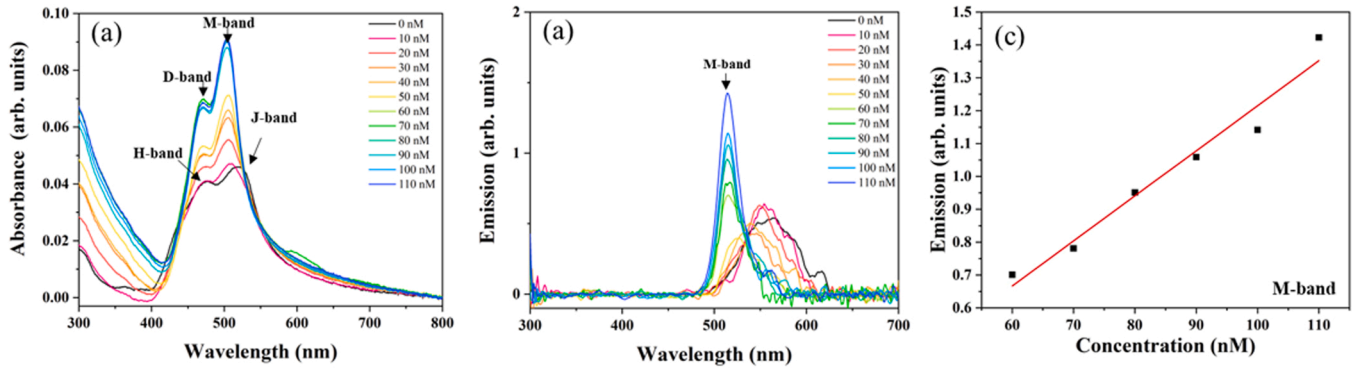

Fig. 8. (a) UV–vis absorption and (b) fluorescence spectra of non-crystalline Davydov-split aggregate particles before and after the addition of BSA with different concentrations. The solution of aggregate particles was diluted by 250 times with synthetic urine. Each spectrum was taken after 4 h incubation with BSA. (c) The plot of the intensity of the turn-on fluorescence at 514 nm (M-band) as a function of BSA concentrations.

band at 474 nm (Fig. 8a). After the addition of 10 nM BSA, a monomer band at 492 nm and a H-dimer band at 466 nm were observed (Fig. 8a), suggesting the disassembly of the Davydov-split aggregate particles. The intensity of the monomer and H-dimer absorption bands increased with the increase of the BSA concentration from 10 nM to 110 nm, in which the monomer band was predominant. The non-crystalline Davydov-split aggregate particles in synthetic urine showed weak fluorescence with a maximum of 570 nm (Fig. 8b). After the addition of BSA, the fluorescence band gradually shifted to 537 nm with the increase of BSA concentrations from 10 nM to 50 nM, which could be assigned the H-dimers. The formation of H-dimers was also evident in the absorption spectra in the BSA concentration range (Fig. 8a). The weak fluorescence of the H-dimers suggested the parallel arrangement of $DiOC_{14}(3)$ molecules. When the BSA concentration increased to 60 nM, the H-dimer emission at 537 nm disappeared. Instead, the monomer emission at 517 nm was observed. Based on the fluorescence spectra, we inferred that the disassembly of non-crystalline Davydov-split aggregate particles in this condition might involve the following:

Aggregate particles + BSA → [H-Dimer/BSA] (1)

[H-Dimer/BSA] + BSA → 2[Monomer/BSA] (2)

After the 250-time dilution, the total concentration of $DiOC_{14}(3)$ in the solution was estimated to be ~ 2 μM. At the beginning of the process, the disassembled $DiOC_{14}(3)$ molecules was in a large excess and complexed with BSA as H-dimers (1). With the increase of BSA concentrations, the H-Dimer/BSA complex disassembled to form the monomer/BSA complex (2). The intensity of the monomer emission at 517 nm linearly increased over the BSA concentration range from 60 nM to 120 nM (Fig. 8c), giving the detection limit of ~ 6 nM, which was comparable to that of the non-fluorescence aggregate nanoparticles reported in the literature [7,9], and lower than the clinical value of the urinary albumin of kidney patients [36]. Although traditional analytical techniques such as immunoassays [37] and liquid chromatography [38] are widely used for the detection of urinary albumin, they often require complicated procedures, expensive reagents and specific instruments. The turn-on fluorescence of non-crystalline Davydov-split aggregate particles are simple and low-cost with the low background fluorescence for the sensitive and selective detection of BSA.

4. Conclusions

We use the self-assembly of $DiOC_{14}(3)$ molecules in the methanol/water mixture to form non-crystalline Davydov-split aggregate particles, which show very weak fluorescence. Through the interaction with BSA, the non-crystalline Davydov-split aggregate particles gradually disassemble. The disassembled $DiOC_{14}(3)$ molecules form the complexes with BSA in the monomer and twisted H-dimer forms, consequently turning on fluorescence. The turn-on fluorescence is highly specific to BSA and increases linearly with the concentration of BSA. We further show that the fluorescence of non-crystalline Davydov-split aggregate particles can also be turned on by BSA in synthetic urine, which increases as the increase of the BSA concentration from 60 nM to 120 nM, giving the detection limit of as low as 6 nM. The protein specific turn-on fluorescence of non-crystalline Davydov-split aggregate particles are potential for the detection of urinary albumin.

CRediT authorship contribution statement

Yiping Ma: Data curation, Validation, Methodology. **Arianna Dicce:** Validation. **Nitin Ramesh Reddy**: Validation. **Jiyu Fang**: Conceptualization, Supervision, Writing.

Declaration of Competing Interest

The authors declare that they have no known competing financial interests or personal relationships that could have appeared to influence the work reported in this paper.

Data Availability

Data will be made available on request.

Acknowledgments

This work was supported by the USA National Science Foundation (CBET 1803690).

References

[1] A. Mishra, R.K. Behera, P.K. Behera, B.K. Mishra, G.B. Behera, Cyanines during the 1990s: a review, Chem. Rev. 100 (2000) 1973–2011.
[2] W. Sun, S. Guo, C. Hu, J. Fan, X. Peng, Recent development of chemosensors based on cyanine platforms, Chem. Rev. 116 (2016) 7768–7817.
[3] Z. Guo, S. Nam, S. Park, J. Yoon, A highly selective ratiometric near-infrared fluorescent cyanine sensor for cysteine with remarkable shift and its application in bioimaging, Chem. Sci. 3 (2012) 2760–2765.
[4] J.A. Carr, D. Franke, J.R. Caram, C.F. Perkinson, M. Saif, V. Askoxylakis, M. Datta, D. Fukumura, R.K. Jain, M.G. Bawendi, O.T. Bruns, Shortwave infrared fluorescence imaging with the clinically approved near-infrared Dye indocyanine green, Proc. Natl. Acad. Sci. U. S. A. 115 (2018) 4465–4470.
[5] S. Zhu, Z. Hu, R. Tian, B.C. Yung, Q. Yang, S. Zhao, D.O. Kiesewetter, G. Niu, H. Sun, A.L. Antaris, X. Chen, Repurposing cyanine NIR-I dyes accelerates clinical translation of near-infrared-II (NIR-II) Bioimaging, Adv. Mater. 30 (2018) 1802546.
[6] R.M. Exner, F. Cortezon-Tamarit, S.I. Pascu, Explorations into the effect of *meso*-substituents in tricarbocyanine dyes: a path to diverse biomolecular probes and materials, Angew. Chem. Int. Ed. 60 (2021) 6230–6241.
[7] P. Anees, S. Sreejith, A. Ajayaghosh, Self-assembled near-infrared dye nanoparticles as a selective protein sensor by activation of a dormant fluorophore, J. Am. Chem. Soc. 136 (2014), 13233−1323.
[8] Y. Yu, Y. Huang, F. Hu, Y. Jin, G. Zhang, D. Zhang, R. Zhao, Self-assembled nanostructures based on activatable red fluorescent dye for site-specific protein probing and conformational transition detection, Anal. Chem. 88 (2016) 6374–6381.
[9] Z. Wang, X. Yan, H. Liu, D. Zhang, W. Liu, C. Xie, Q. Li, J. Xu, A. Novel, Hydrazide schiff base self-assembled nanoprobe for selective detection of human serum albumin and its applications in renal disease surveillance, J. Mater. Chem. B 8 (2020) 8346–8355.
[10] X. Fan, Q. He, S. Sun, H. Li, Y. Pei, Y. Xu, Nanoparticles self-assembled from multiple interactions: a novel near-infrared fluorescent sensor for the detection of serum albumin in human sera and turn-on live-cell imaging, Chem. Commun. 52 (2016) 1178–1181.
[11] Z. Zheng, H. Li, S.H.S. Sun, Y. Xu, Media dependent switching of selectivity and continuous near infrared turn-on fluorescence response through cascade interactions from noncovalent to covalent binding for detection of serum albumin in living cells, ACS Appl. Mater. Interfaces 10 (2018) 44336–44343.
[12] F. Würthner, T.E. Kaiser, C.R. Saha-Möller, J-aggregates: from serendipitous discovery to supramolecular engineering of functional dye, Mater. Angew. Chem. Int. Ed. 50 (2011) 3376–3410.
[13] E.E. Jelley, Spectral absorption and fluorescence of dyes in the molecular state, Nature 138 (1936) 1009–1010.
[14] F.C. Spano, The spectral signatures of frenkel polarons in H- and J-aggregates, Acc. Chem. Res. 43 (2010) 429–439.
[15] A.S. Davydov, Theory of Molecular Excitons, Plenum press, New York, 1971.
[16] B.L. Cannon, L.K. Patten, D.L. Kellis, P.H. Davis, J. Lee, E. Graugnard, B. Yurke, W. B. Knowlton, Large davydov splitting and strong fluorescence suppression: an investigation of exciton delocalization in DNA-templated holliday junction dye aggregates, J. Phys. Chem. A. 122 (2018) 2086–2095.
[17] C. Zhong, D. Bialas, C.J. Collison, F.C. Spano, Davydov splitting in squaraine dimers, J. Phys. Chem. C. 123 (2019) 18734–18745.
[18] N.R. Reddy, S. Rhodes, Y. Ma, J. Fang, Davydov split aggregates of cyanine dyes on self-assembled nanotubes, Langmuir 36 (2020) 13649–13655.
[19] L.I. Markova, V.L. Malinovskii, L.D. Patsenker, R. Haner, J-vs. H-type assembly: pentamethine cyanine (Cy5) as a Near-IR chiroptical reporter, Chem. Commun. 49 (2013) 5298–5300.
[20] M. Pajusalu, M. Raetsep, G. Trinkunas, A. Freiberg, Davydov splitting of excitons in cyclic bacteriochlorophyll a nanoaggregates of bacterial light-harvesting complexes between 4.5 and 263 K, ChemPhysChem 12 (2011) 634–644.
[21] N.R. Reddy, M. Aubin, A. Kushima, J. Fang, Fluorescent H-aggregate vesicles and tubes of a cyanine dye and their potential as light-harvesting antennae, J. Phys. Chem. B. 125 (2021) 7911–7918.
[22] H. Sun, J. Xiang, X. Zhang, H. Chen, Q. Yang, Q. Li, A. Guan, Q. Shang, Y. Tang, G. A. colorimetric and fluorometric dual-modal supramolecular chemosensor and its application for HSA detection, Analyst 139 (2014) 581–584.
[23] A.K. Chibisov, G.V. Zakharova, H. Görner, Photoprocesses in dimers of thiacarbocyanines, Phys. Chem. Chem. Phys. 1 (1999) 1455–1460.
[24] S. Chakraborty, P. Debnath, D. Dey, D. Bhattacharjee, S.A. Hussain, Formation of fluorescent H-aggregates of a cyanine dye in ultrathinfilm and its effect on energy transfer, J. Photochem. Photobio. A 293 (2014) 57–64.
[25] Y. Ma, A. Dicce, N.R. Reddy, J. Fang, Liquid-crystalline ordering of davydov-split aggregates of cyanine dyes, Colloids Surf. A. 642 (2022) 28713.
[26] Th Peters. Jr, All About Albumin, Academic Press, San Diego, 1996.
[27] X.M. He, D.C. Carter, X.M. He, D.C. Carter, Atomic structure and chemistry of human serum albumin, Nature 358 (1992) 209–215.
[28] A.S. Tatikolov, S.M.B. Costa, Complexation of polymethine dyes with human serum albumin: a spectroscopic study, Biophys. Chem. 107 (2004) 33–49.
[29] K. Awasthi, G. Nishimura, Modification of near-infrared cyanine dyes by serum albumin protein, Photochem. Photobiol. Sci. 10 (2011) 461–463.
[30] D.S. Pisoni, L. Todeschini, A.C.A. Borges, C.L. Petzhold, F.S. Rodembusch, L. F. Campo, Symmetrical and asymmetrical cyanine dyes. synthesis, spectral properties, and BSA association study, J. Org. Chem. 79 (2014) 5511–5520.
[31] P.R. Patlolla, N. Desai, S. Gupta, B. Datta, Interaction of a dimeric carbocyanine dye aggregate with bovine serum albumin in non-aggregated and aggregated forms, Spectrochim. Acta A. 209 (2019) 256–263.
[32] R. Tian, Q. Zeng, S. Zhu, J. Lau, S. Chandra, R. Ertsey, K.S. Hettie, T. Teraphongphom, Z. Hu, G. Niu, D.O. Kiesewetter, H. Sun, X. Zhang, A.L. Antaris, B.R. Brooks, X. Chen, Albumin-chaperoned cyanine dye yields superbright NIR-II fluorophore with enhanced pharmacokinetics, Sci. Adv. 5 (2019) eaaw0672.

[33] U. Rosch, S. Yao, R. Wortmann, F. Wurthner, Fluorescent H-aggregates of merocyanine dyes, Angew. Chem. Int. Ed. 45 (2006) 7026–7030.
[34] N. Ryu, Y. Okazaki, E. Pouget, M. Takafuji, S. Nagaoka, H. Ihara, R. Oda, Fluorescence emission originated from the H-aggregated cyanine dye with chiral gemini surfactant assemblies having a narrow absorption band and a remarkably large stokes shift, Chem. Commun. 53 (2017) 8870–8873.
[35] Y. Zhang, J. Xiang, Y. Tang, G. Xu, W. Yan, Chiral transformation of achiral J-aggregates of a cyanine dye templated by human serum albumin, ChemPhysChem 8 (2007) 224–226.
[36] J.E. Bennett, D.J. Rowe, R.W. Morris, W. Gatling, K.M. Shaw, A. Polak, Assessment of immunochemical methods for determining low concentrations of albumin in urine, Clin. Chem. 32 (1986) 1544–1548.
[37] M.J. Doyle, H.B. Halsall, W.R. Heineman, Heterogeneous immunoassay for serum proteins by differential pulse anodic stripping voltammetry, Anal. Chem. 54 (1982) 2318–2322.
[38] F. Eertmans, V. Bogaert, B. Puype, Development and validation of a high-performance liquid chromatography (HPLC) method for the determination of human serum albumin (HSA) in medical devices, Anal. Methods 3 (2011) 1296–1302.